The Rift Valley fever accessory proteins NSm and P78/NSm-GN are distinct determinants of virus propagation in vertebrate and invertebrate hosts.

Felix Kreher, Carole Tamietti, Céline Gommet, Laurent Guillemot, Myriam Ermonval, Anna-Bella Failloux, Jean-Jacques Panthier, Michèle Bouloy, Marie Flamand

OPEN

Emerging Microbes and Infections (2014) 3, e71; doi:10.1038/emi.2014.71

www.nature.com/emi

ORIGINAL ARTICLE

The Rift Valley fever accessory proteins NSm and P78/NSm-G_N are distinct determinants of virus propagation in vertebrate and invertebrate hosts

Felix Kreher[1,2,3], Carole Tamietti[1,2], Céline Gommet[4,5,6,*], Laurent Guillemot[4,5,*], Myriam Ermonval[1,*], Anna-Bella Failloux[7], Jean-Jacques Panthier[4,5], Michèle Bouloy[1] and Marie Flamand[1,2]

Rift Valley fever virus (RVFV) is an enzootic virus circulating in Africa that is transmitted to its vertebrate host by a mosquito vector and causes severe clinical manifestations in humans and ruminants. RVFV has a tripartite genome of negative or ambisense polarity. The M segment contains five in-frame AUG codons that are alternatively used for the synthesis of two major structural glycoproteins, G_N and G_C, and at least two accessory proteins, NSm, a 14-kDa cytosolic protein, and P78/NSm-G_N, a 78-kDa glycoprotein. To determine the relative contribution of P78 and NSm to RVFV infectivity, AUG codons were knocked out to generate mutant viruses expressing various sets of the M-encoded proteins. We found that, in the absence of the second AUG codon used to express NSm, a 13-kDa protein corresponding to an N-terminally truncated form of NSm, named NSm′, was synthesized from AUG 3. None of the individual accessory proteins had any significant impact on RVFV virulence in mice. However, a mutant virus lacking both NSm and NSm′ was strongly attenuated in mice and grew to reduced titers in murine macrophages, a major target cell type of RVFV. In contrast, P78 was not associated with reduced viral virulence in mice, yet it appeared as a major determinant of virus dissemination in mosquitoes. This study demonstrates how related accessory proteins differentially contribute to RVFV propagation in mammalian and arthropod hosts.
Emerging Microbes and Infections (2014) **3,** e71; doi:10.1038/emi.2014.71; published online 1 October 2014

Keywords: arbovirus; attenuation; bunyavirus; transmission; minor structural protein; non-structural protein; vector; virulence factor

INTRODUCTION

Rift Valley fever virus (RVFV), which is enzootic in Africa, was first isolated in 1930 during a major outbreak in Kenya.[1,2] RVF manifestations were initially recognized through numerous abortions in pregnant ewes and a high mortality rate in young animals.[1] Over the past decades, recurrent outbreaks of this virus have occurred mostly in sub-Saharan countries, such as Madagascar and Egypt.[3–5] The recent introduction of the virus into the Arabian Peninsula has raised concerns for a possible spread of the virus throughout southern Europe.[6,7] RVFV can be transmitted to its hosts during feeding of a mosquito vector or by direct contact with contaminated fluids.[8–10] The disease in humans is most commonly a self-limited, flu-like syndrome, but manifestations such as hepatitis, jaundice, retinitis, meningo-encephalitis or signs of hemorrhages are frequently observed in the severe forms of RVF.[3,9,11–13] The overall fatality rate in humans usually remains below 1%, although this rate has exceeded 10% in recent epidemics.[3,10]

RVFV belongs to the family *Bunyaviridae*, which is divided into five genera (*Orthobunyavirus*, *Nairovirus*, *Phlebovirus*, *Hantavirus* and *Tospovirus*). The family comprises major human pathogens such as hantavirus (*Hantavirus*), Crimean-Congo hemorrhagic fever virus (*Nairovirus*), RVFV and severe fever with thrombocytopenia syndrome virus (*Phlebovirus*).[14] RVFV is an enveloped virus containing a tripartite RNA genome of negative or ambisense polarity.[15,16] The L segment codes for the RNA-dependent RNA polymerase, and the S segment utilizes an ambisense strategy to express the nucleoprotein N and non-structural protein NSs, which is a major virulence factor. The M segment is composed of one large open reading frame that encodes the two envelope glycoproteins G_N and G_C and contains an additional upstream NSm region, the translation of which depends on the alternative usage of five in-frame AUG codons (Figure 1A).[15]

Translational products of the M segment have been characterized *in vitro* and consist of a nested set of polyproteins that are expressed from different AUG codons, presumably through a leaky scanning mechanism. The polyprotein precursors are then cleaved by cellular signalases to generate the individual proteins.[17–19] Initiation of translation at the first AUG codon leads to synthesis of a NSm–G_N–G_C precursor that contains a signal sequence upstream of NSm, which allows for translocation of the polyprotein into the endoplasmic reticulum (Figure 1B).[11] In this context, cleavage only occurs after the NSm and G_C signal peptides, leading to the release of a 78-kDa glycoprotein, namely, P78, NSm1 or the large glycoprotein, which consists of an NSm–G_N fusion protein.[11] G_C is cleaved from the precursor, but may be highly unstable in the absence of a functional G_N. Initiation of translation from AUG 2 takes place downstream of the signal sequence of NSm such that the

[1]Molecular Genetics of Bunyaviruses, Institut Pasteur, F-75015 Paris, France; [2]Structural Virology, Institut Pasteur, F-75015 Paris, France; [3]Univ Paris Diderot, Sorbonne Paris Cité, F-75205 Paris, France; [4]Mouse Functional Genetics, Institut Pasteur, F-75015 Paris, France; [5]CNRS URA 2578, Institut Pasteur, F-75015 Paris, France; [6]Central Animal Facilities, Institut Pasteur, F-75015 Paris, France and [7]Arboviruses and Insect Vectors, Institut Pasteur, F-75015 Paris, France
*Present address: Gommet Céline: CEA, ImmunoVirology Department, DSV/iMETI, Fontenay-aux-Roses, F-92260 Paris, France; Guillemot Laurent: Innate Host Defense and Inflammation, Institut Pasteur, F-75015 Paris, France; Ermonval Myriam: Antiviral strategies, Institut Pasteur, F-75015 Paris, France.
Correspondence: M Flamand
E-mail: marie.flamand@pasteur.fr
Received 9 June 2014; revised 5 August 2014; accepted 10 August 2014

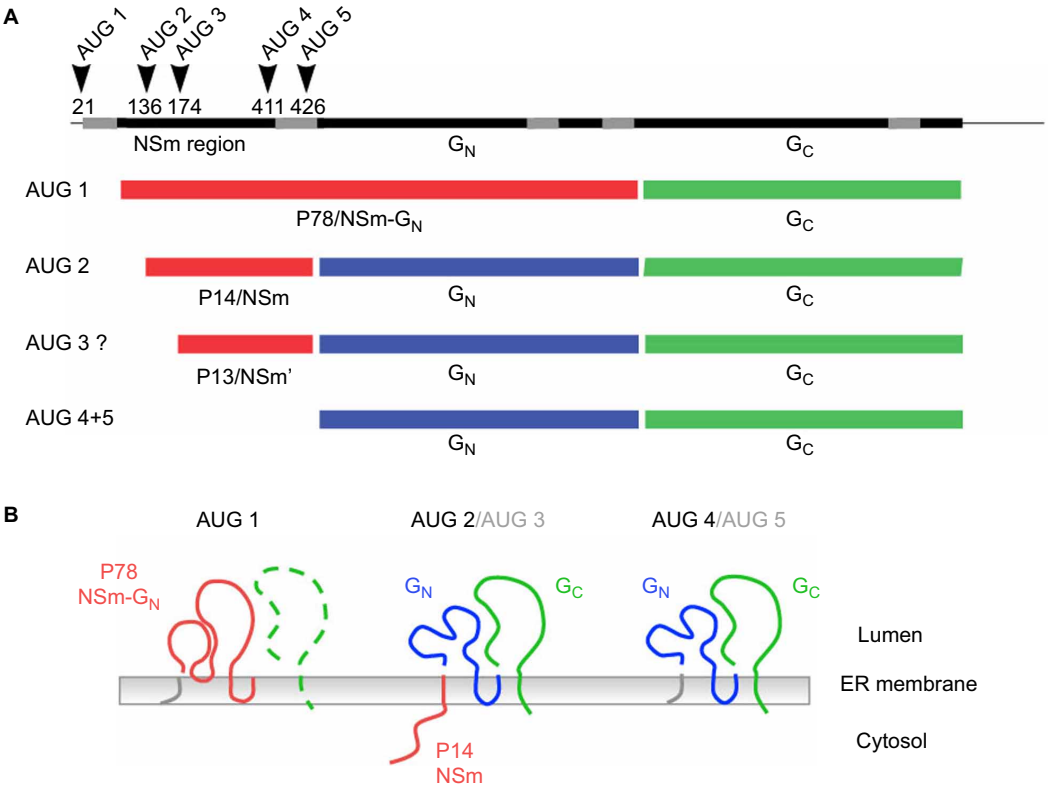

C

	P78	P14	P13	G_N	G_C
rWT	+	+	+	+	+
AUG 1 KO	–	+	+	+	+
AUG S1 KO	–	+	+	+	+
AUG 2 KO	+	–	+	+	+
AUG 3 KO	+	+	–	+	+
AUG 1+2 KO	–	–	+	+	+
AUG 1+3 KO	–	+	–	+	+
AUG 2+3 KO	+	–	–	+	+
AUG 4+5 KO	+	+	+	+	+
AUG 1+2 KO NSm'-V5	–	–	+	+	+
AUG 1+2+3 KO	–	–	–	+	+
AUG S1+2+3 KO	–	–	–	+	+

Figure 1 Description of the different proteins encoded by the RVFV M segment. (**A**) Schematic representation of the RVFV M segment in the antigenomic orientation. The relative nucleotide position of the different in-frame AUG codons in the NSm region and the coding regions of NSm, G_N and G_C are depicted on the upper graph. Transmembrane domains are indicated as gray rectangles. This panel also shows the schematic representation of the polypeptides expressed from each of the AUG codons. Different proteins, including P78 and NSm (red), G_N (blue) and G_C (green), are generated upon cleavage of polyprotein precursors. (**B**) Model of protein topology in the context of different AUG usage. (**C**) Description of the AUG KO mutant viruses produced during this study, with their corresponding protein expression profiles. ER, endoplasmic reticulum.

NSm amino-acid sequence remains on the cytosolic side of the membrane and only the two structural glycoproteins, G_N and G_C, enter the lumen of the endoplasmic reticulum (Figure 1B).[15] Cleavage of this NSm–G_N–G_C precursor occurs after the signal sequences of G_N and G_C, giving rise to NSm, a 14-kDa protein that was initially referred to as NSm2, in addition to the G_N and G_C proteins (Figure 1B).[15] AUG 4 and AUG 5, which are localized downstream of the NSm region, also contribute to G_N and G_C expression, while AUG 3 does not seem to play a significant role in translation initiation.[19]

The P78 glycoprotein localizes to the Golgi complex.[20] It has been found to form heterodimers with the G_C envelope protein and to co-sediment with virus or virus-like particles.[21–24] A recent report shows an association of this protein with virus particles produced from C6/36 mosquito cells but not from simian Vero E6 cells infected with RVFV, suggesting an important role of P78 in the insect vector.[25] Although the cytosolic non-structural NSm protein shares the same amino-acid sequence with the N-terminal portion of P78, it has a very different fate from its glycoprotein counterpart. NSm is specifically targeted to the outer membrane of mitochondria, where it may impede activation of the apoptotic cascade and regulate the p38 mitogen-activated protein kinase response.[26] Neither P78 nor NSm are required during viral replication in mammalian (Vero or MRC5) or mosquito (C6/36) cell cultures.[27,28] However, a recombinant RVFV deleted of the full NSm region, which accordingly lacks expression of the two accessory

proteins, is highly attenuated in rats and shows a reduced ability to infect mosquitoes.[29–31]

A detailed functional analysis using mice and mosquitoes as experimental models is now needed to specify the role of the different M-encoded accessory proteins during virus infection of vertebrate and invertebrate hosts. To this end, we generated a set of mutant viruses in which one or several AUGs in the M segment were knocked out (KO) (Figure 1C). We found that NSm is an important determinant of RVFV virulence in mice, while P78 plays no apparent role in this animal model. In contrast, mutant viruses that lack expression of P78 show poor to no dissemination in the mosquito vector. In agreement with these observations, we observed that the respective AUG KO mutant viruses replicate to substantially lower levels in murine macrophages and mosquito cells cultured *in vitro*.

MATERIALS AND METHODS

Cell lines

Baby hamster kidney cells stably expressing T7 polymerase (BHK/T7-9)[32] (kindly provided by Naoto Ito Gifu, Japan) were cultured in minimum essential medium supplemented with 10% fetal calf serum (FCS; Biowest, Nuaillé, France) and Tryptose phosphate broth. Vero E6 cells (kindly provided by Stephen Goodbourn, London, UK) were grown in Dulbecco's modified Eagle's medium (DMEM) (Gibco, Life Technologies, Cergy-Pontoise, France) supplemented with 10% FCS. Murine fibroblastic L929 cells and murine macrophage RAW 264.7 cells (ATCC, LGC Standards, Molsheim, France) were cultured in DMEM supplemented with *L*-glutamine and 10% FCS. Mammalian cells lines were maintained at 37 ℃ under 5% CO_2 in medium supplemented with 10 IU of penicillin and 10 μg of streptomycin per mL. *Aedes albopictus*-derived C6/36 cells were grown in Leibowitz's L-15 medium (Gibco, Life Technologies, Cergy-Pontoise, France) supplemented with 10% FCS (Lonza, Verviers, Belgium) and 2% Tryptose phosphate broth (Sigma-Aldrich, Lyon, France) and incubated at 28 ℃ without CO_2.

Plasmids

Plasmids containing the L, M or S segments of RVFV (ZH548 strain) located downstream of the Pol-l promoter in pRF108 have been described.[33] pRF108-M, which encodes the M segment, was used to generate single AUG-to-GCG mutations or combinations of KO mutations by site-directed mutagenesis. The mutants were sequenced for the presence of the targeted mutations as well as the absence of additional mutations. The viral proteins N and L were expressed under the control of the T7 promoter/terminator and encephalomyocarditis virus internal ribosomal entry site using the pTM1 plasmid.

Virus production

RVFV was rescued by transfecting BHK/T7-9 cells as previously described.[33] Briefly, cells were transfected using Fugene6 reagent (Roche Diagnostics, Meylan, France) according to the manufacturer's instructions using a ratio of Fugene6 to plasmid DNA of 3 μL/μg of pTM1-N, pTM1-L and pRF108-L, -M and -S. Medium was collected 3–5 days post-transfection, stored at −80 ℃ and used to produce virus stocks. The NSm region of the M segment was then entirely sequenced. Subconfluent monolayers of Vero E6 cells were infected with RVFV ZH548 or recombinant viruses at a multiplicity of infection (MOI) of 0.01 in DMEM supplemented with 2% FCS and antibiotics. The medium was collected when a cytopathic effect was observed at approximately 72 h post-infection (PI). Supernatants were clarified and stored at −80 ℃. Virus was titrated via plaque assay on Vero E6 cells incubated under a 1% agarose layer for 3–4 days at 37 ℃, and plaques were stained with a crystal violet solution at 0.2% in 10% formaldehyde and 20% ethanol.

Virus stability

Viruses were passaged on confluent Vero E6 cells infected at a MOI of 0.01 to follow the emergence of compensatory mutations over five sequential rounds of infections. RNA was extracted from infected cells at each passage using TRIzol reagent (Invitrogen, Life Technologies) according to the manufacturer's instructions. 3′-rapid amplification of cDNA ends (3′ RACE) was then carried out using a poly(A) polymerase tailing kit (Epicentre Biotechnologies, Tebu-Bio, Le Perray en Yvelines, France). Briefly five micrograms of total RNA was polyadenylated in a 20-μL reaction mixture for 7 min at 37 ℃. The RNA was then purified, and reverse transcription was carried out using the oligo(dT) 3′ RACE-adaptor primer (AP) (Invitrogen) or primers specific for the M segment and avian myeloblastosis virus reverse transcriptase (RT) (Promega, Charbonnières, France). This step was followed by polymerase chain reaction (PCR) using the KOD polymerase (Toyobo, Merk, Darmstadt, Germany) and specific primers and/or 3′ RACE-AP. The resulting RT-PCR products were separated by agarose electrophoresis, and the DNA bands with the correct sizes were purified using the QIAquick purification kit (Qiagen, Courtaboeuf, France) and then sequenced according to standard protocols using the BigDye terminator v1.1 kit (Applied Biosystems, Villebon-sur-Yvette, France).

Western blotting

Infected cells were washed with phosphate buffered saline (PBS) and lysed using NET buffer containing 1% (v/v) Triton X-100, 0.5% sodium dodecyl sulfate (SDS) and protease inhibitors (Complete Protease Inhibitor; Roche) and incubated 5 min on ice. The cell lysates were centrifuged at 10 000*g* for 10 min, and a jelly-like pellet containing mostly DNA was removed. The protein content was quantified using a micro-BCA test (Thermo Fischer Scientific, Illkirch, france), and equal amounts of total proteins were loaded onto 10% or 12% SDS–polyacrylamide gels (BioRad, Marnes-la-Coquette, France) in reducing conditions. The proteins were then transferred onto nitrocellulose membranes (Amersham, GE Healthcare Europe GmbH, Velizy-Villacoublay, France). The membranes were blocked with a solution of 5% dried skim milk in PBS containing 0.05% Tween 20, which was also used to dilute the antibodies (Abs). The 4D4 mouse monoclonal antibody (Ab) (kindly provided by Dr C Schmaljohn) was used to detect G_N. The N protein was detected using a rabbit polyclonal Ab raised against a recombinant protein produced in the baculovirus system, and NSm-related proteins were detected using a rabbit polyclonal Ab directed against a peptide corresponding to the 13 amino acids downstream of AUG 2 (MC14) (MIEGAWDSLREEE). V5-tagged proteins were detected using an anti-V5 Ab (Invitrogen). Immunodetection was performed by incubating the membranes with an anti-mouse or anti-rabbit Ab coupled to horseradish peroxidase (Sigma-Aldrich) followed by incubation with a chemiluminescent substrate (ECL Pierce/Thermo Fischer Scientific). Signals were detected by film exposure (Amersham) or using a G-box (Ozyme, Montigny-Le-Bretonneux, France).

Immunofluorescence microscopy

Cells grown for 24 h on coverslips were infected with wild type (WT) or mutant viruses. The infected cells were then fixed at the indicated time PI with 3.7% formaldehyde in PBS for 30 min at room temperature, permeabilized with 0.05% TritonX-100 for 10 min and then saturated with PBS containing 3% FCS and 0.05% Tween 20 for 30 min. The Abs were diluted in PBS containing 3% FCS and 0.05% Tween 20 and incubated 1 h at room temperature. The same Abs as those used for Western blotting were used for the detection of G_N, N protein, NSm-related proteins and V5; and TOM22 was detected using an anti-TOM22

mouse monoclonal Ab (Sigma-Aldrich, Lyon, France). Alexa Fluor 555- and Alexa Fluor 488-conjugated goat anti-mouse or anti-rabbit Abs were used as secondary Abs (Molecular Probes, Life Technologies). Image acquisition was performed with a Zeiss Axiovert 200M inverted microscope (Imagopole; Institut Pasteur, Paris, France). A series of grid-projection acquisitions allowed for optical slice view reconstruction using the Zeiss Axiovision 4.8 software.

Mouse virulence assays

Inbred female C57BL/6J mice were purchased from Charles River Laboratories (L'Arbresle, France). Groups of 8-week-old mice were inoculated intraperitoneally with 100 plaque-forming units (PFU) of RVFV and kept in biosafety level 3 isolators, as previously described.[34] The morbidity, mortality and clinical disease scores of the mice were monitored daily for 14 days following infection. Mice that showed signs of illness, i.e., ruffled fur and hunched posture, were euthanized. Animals that survived were euthanized on the last day of the monitoring period.

Mosquito infections

Seven-day-old F1 female *Aedes aegypti* mosquitoes were infected with concentrated preparations of virus. To this end, confluent layers of Vero E6 cells were infected at an MOI of 0.1. At 72 h PI, cell culture supernatants were collected, and cellular debris was eliminated by centrifugation at 1500*g* for 10 min at 4 ℃. Supernatants were incubated for 4 h with 7.5% (w/v) PEG 6000, and virus particles were pelleted at 10 000*g* for 45 min at 4 ℃. The virus pellets were resuspended in a 20% sucrose solution in PBS (w/v), and the viruses were then loaded onto a 20 to 60% sucrose gradient and centrifuged at 190 000*g* for 12 h at 4 ℃. Virus was dialyzed against PBS for 8 h at 4 ℃, and titers were determined using plaque assays. The Hemotek feeding system was used to provide an infectious blood meal, which was composed of a virus suspension supplemented with washed rabbit erythrocytes and adenosine triphosphate (ATP) (5 mM) at a titer of 6.6×10^7 PFU/mL, at 37 ℃ to the mosquitoes. Fully engorged females were transferred in cardboard containers and maintained with 10% sucrose at 28±1 ℃ for 14–21 days. Virus infection and dissemination rates in mosquito heads and bodies, respectively, which were homogenized in a bead beater in 300 µL of DMEM were evaluated by plaque assays.

Ethics statement

Experiments on live mice were conducted according to the French and European regulations on care and protection of laboratory animals (EC Directive 86/609, French Law 2001-486 issued on 6 June 2001) and the National Institutes of Health Animal Welfare (Insurance #A5476-01 issued on 2 July 2007). Experimental protocols were approved by the Animal Ethics Committee #1 of the Comité Régional d'Ethique pour l'Expérimentation Animale, Ile de France (NO 2012-0025) and carried out in compliance with the Institut Pasteur Biosafety Committee.

RESULTS

Production and characterization of AUG KO mutant RVFV

To evaluate the relative impact of the NSm-related proteins on viral virulence, we used site-directed mutagenesis to generate a set of single, double and triple AUG KO mutations in the RVFV M segment and used a reverse genetics system to rescue the infectious WT ZH548 strain and its derived mutants (Figure 1C).[33] Viruses carrying the WT or AUG mutants of the M segment were rescued in BHK/T7-9 cells, and viral stocks were produced on Vero E6 cells. All viruses were analyzed for G_N and N expression in infected Vero E6 cells (data not shown) by immunofluorescence (IF). Consistent with previous reports, no significant differences could be observed between mutant and WT virus-infected cells.[27,28] Cell lysates from infected Vero E6 cells were further analyzed by Western blotting (Figure 2A), which showed that all viruses expressed the viral proteins G_N and N to similar levels. We also used anti-NSm Abs generated against a peptide corresponding to the 14 amino acids downstream of AUG 2 (MC14) to ascertain the presence or absence of the P78 and NSm proteins in cells infected by the different mutant viruses. As previously reported, we found that the expression of P78 and NSm depended on the first and second AUG codons, respectively. Surprisingly, using sodium dodecyl sulfate polyacrylamide gel electrophoresis (SDS-PAGE), we found that NSm migrated at a higher apparent molecular weight in all mutants that carried AUG 2 but were mutated at AUG 3 (AUG 3 KO and AUG 1+3 KO). The type of post-translational processing that accounts for this difference in migration is unclear.

Expression of an NSm′ protein from the AUG 3 start site

The anti-NSm antibody was not initially designed to detect the N-terminally truncated form of the NSm protein that may be expressed from AUG 3 (the MC14 epitope lies upstream of AUG 3). To demonstrate that an NSm′ protein can be synthesized from AUG 3, a V5 tag was introduced downstream of AUG3 in the backbone of an AUG 1+2 KO mutant virus (Figure 2B). This virus expressed viral proteins G_N and N, as shown by IF analysis of infected cells. Lysates from the cells infected with the AUG 1+2 KO/NSm′-V5 mutant virus were analyzed by Western blotting with a V5-specific Ab. Two bands specific to V5-tagged proteins were detected: the most prominent one at approximately 14 kDa represented NSm′ fused to the V5 tag, and a minor band at approximately 75 kDa corresponded to the NSm′-V5-G_N precursor (Figure 2B). The uncleaved NSm'-G_N precursor produced from AUG 3 had been previously described,[26] but the present results show that a cleaved, N-terminally truncated version of the 13-kDa NSm′ protein is preferentially produced in RVFV-infected cells.

Association of NSm and NSm′ with mitochondria

It was recently reported that NSm is a C-terminally anchored protein that is situated on the outer surface of mitochondria.[35] Using the MC14 Ab, we found that NSm expressed in Vero E6 cells infected with the AUG 1 KO virus colocalized exclusively with the mitochondrial marker TOM22 (Figure 3A). This analysis also showed that, in cells infected with an AUG 1+3 KO mutant virus, which leads to an altered migration profile of NSm in polyacrylamide gels, mitochondrial targeting of the viral protein was not compromised. Moreover, the subcellular localization of NSm' fused to a V5-tag was analyzed by IF, and just like the full-length NSm protein, the V5-tagged protein appeared to colocalize with the mitochondrial marker TOM22 (Figure 3B), which indicates that the region between AUG 2 and AUG 3 is not essential for the subcellular localization of NSm.

Stability of the mutant viruses in mammalian cell culture

Before testing the different mutant viruses in an *in vivo* model, we assessed their stability in cell culture (Supplementary Figure S1). To this end, Vero E6 cells were infected at an MOI of 0.01, and supernatants were used to infect new cell monolayers. These infection cycles were repeated several times. RNA was recovered from cells infected by mutant viruses submitted to five rounds of amplification (passage 5), and the entire NSm coding region was sequenced. No reversion of any of the introduced mutations was found. To sequence the

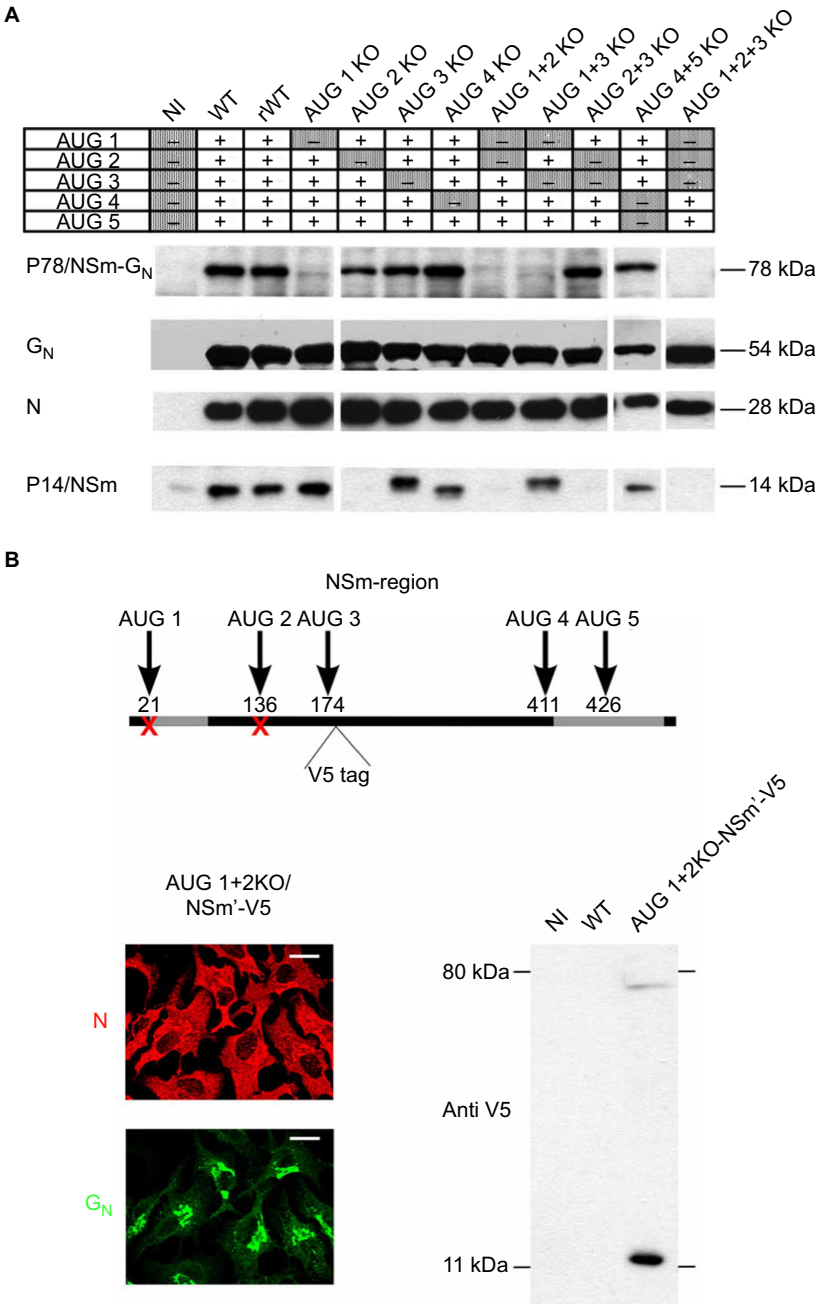

Figure 2 Characterization of protein translation products from AUG 1, 2 and 3 of the M segment. (**A**) Vero E6 cells were either mock-infected or infected at an MOI of 3 with WT ZH548 virus or with the different AUG KO mutant viruses. Protein lysates recovered at 16 h PI were subjected to Western blot analysis. G_N and N were detected with specific Abs, and P78 and NSm were detected with the anti-MC14 Ab. (**B**) IF and Western blotting analysis of NSm′-V5. Representation of the 3′ end of the M segment of the recombinant AUG 1+2 KO NSm′-V5 virus. The different AUG codons are indicated by arrows, and their nucleotide positions are given. AUG codons that were knocked out are marked by a red cross. The position of the inserted V5-tag immediately downstream of AUG 3 is indicated. Signal sequences appear in gray. For the IF analysis, Vero E6 cells were infected with the AUG 1+2 KO NSm′-V5 mutant virus at an MOI of 3. Cells were fixed 16 h PI and stained with Abs specific for the viral proteins G_N and N. Scale bars represent 20 μm. For the Western blot analysis, Vero E6 cells were either mock-infected or infected with the WT ZH548 virus or infected with the AUG 1+2 KO NSm′-V5 mutant virus, and the cell lysates were analyzed with an anti-V5 Ab. The molecular weight and position of the marker bands are indicated (right panel).

3′-untranslated region of the genomic M segment, i.e., upstream of AUG 1 at position 21, 3′ RACE followed by RT-PCR was carried out. Interestingly, we found that a new AUG codon upstream of the mutated AUG 1 was generated through a change of cytosine to uracil at position 10 in the non-coding region (C10U) of the AUG 1 KO, AUG 1+2 KO and AUG 1+3 KO mutant viruses that were sequenced at passage 5 (Supplementary Figure S1A). Analysis of the RNA from the AUG 1 KO mutant at earlier passages revealed a rapid accumulation of the C10U mutation between passages 4 and 5 (Supplementary Figure S1A). In contrast, this AUG codon was not present in the WT nor in the AUG 1+2+3 KO viral RNAs that were recovered at passage 5. This new in-frame AUG codon was positioned only two codons

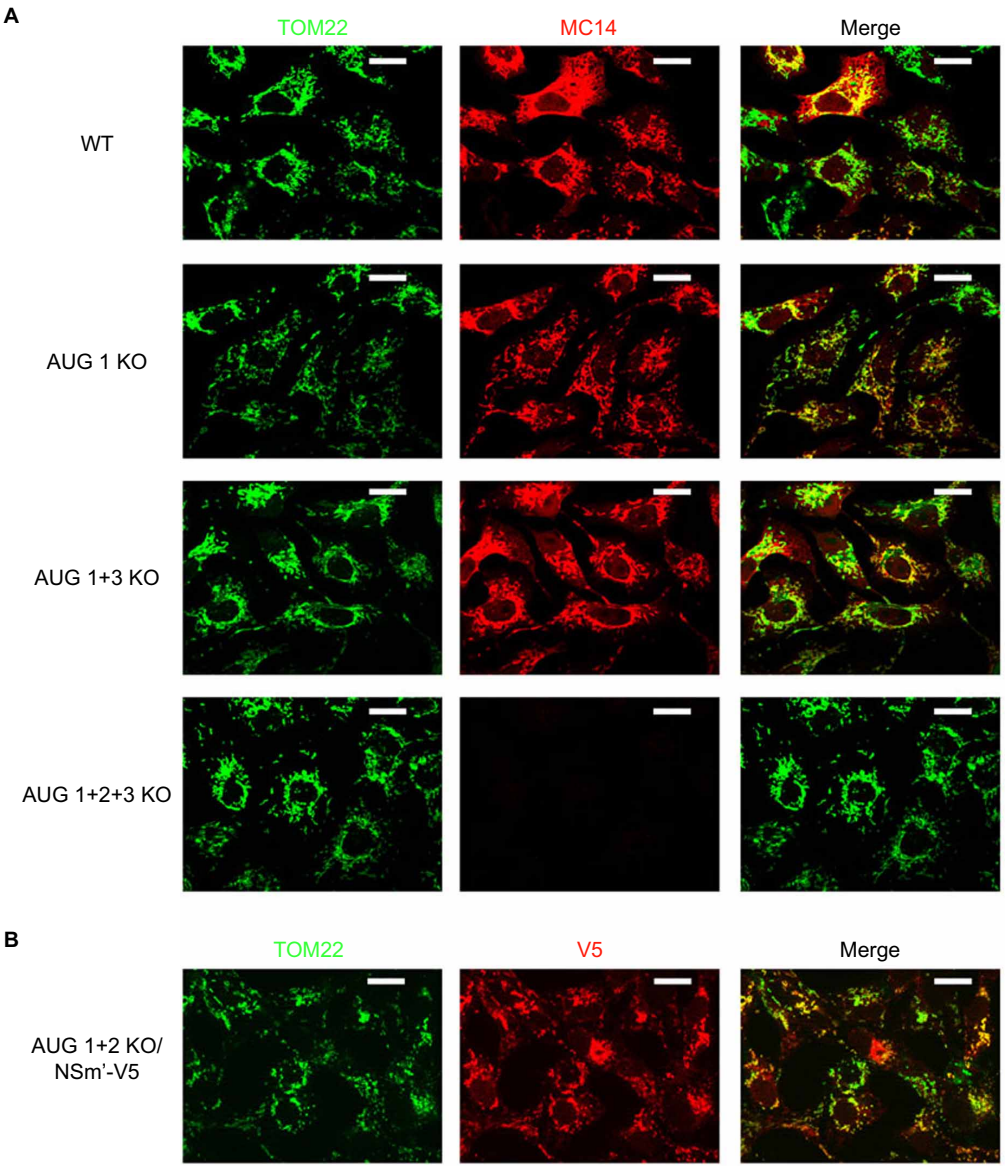

Figure 3 Subcellular localization of the NSm and NSm′ accessory proteins. (**A**) Vero E6 cells infected with either WT ZH548 virus or different AUG KO mutant viruses were fixed 16 h PI and stained with specific antibodies for the mitochondrial marker TOM22 and the anti-NSm MC14 Ab. Colocalization of the two signals is indicated by a yellow label in the merged images. (**B**) Vero E6 cells were either infected with the AUG 1+2 KO NSm′-V5 virus at an MOI of 3. Cells were fixed 16 h PI and stained with specific Abs for TOM22 (green) and V5 (red). Scale bars represent 20 μm.

upstream of a stop codon. However, Western blotting analysis of Vero E6 cells infected with AUG 1 KO virus from either the original stock or passage 5 showed that P78 could be expressed, albeit to a lower extent, from the newly introduced initiation site (Supplementary Figure S1B), suggesting that the in-frame stop codon is too close to the initiation codon to be recognized. To stabilize the KO of AUG 1 in subsequent studies, a mutant virus was produced in which two additional stop codons were introduced at positions 94 and 115, downstream of the predicted P78 signal sequence. These mutations were designed to block any translation initated from an AUG codon introduced upstream of AUG 1 that would restore P78 protein expression. This AUG S1 KO virus was passaged up to eight times, as previously described, and analyzed for the introduction of the C10U mutation. No mutation in the 3′-untranslated region could be detected for the AUG S1 KO virus (data not shown).

Impact of the NSm-related proteins on viral virulence in mice

Various strains of mice have been found to be highly susceptible to infections by RVFV and to display a similar pattern of symptoms as in the severe forms of the disease in humans.[13,34,36] To analyze the impact of the different NSm-related proteins on viral virulence, we conducted an initial animal test in 8-week-old female C57BL/6 mice using mutant viruses in which single AUG codons were knocked out. Mice were injected intraperitoneally with 100 PFU of *in vitro*-reconstituted WT virus (ZH548) or the different mutant viruses, and the mice were monitored for 3 weeks (Figures 1C and 4A). No significant changes in the mice infected with the mutant viruses compared to those infected with the rescued WT virus, neither in time of death nor in survival rates, could be observed. This finding was unexpected because a previous report showed strong attenuation of a RVFV lacking the NSm region in rats.[29] To investigate whether attenuation in mice

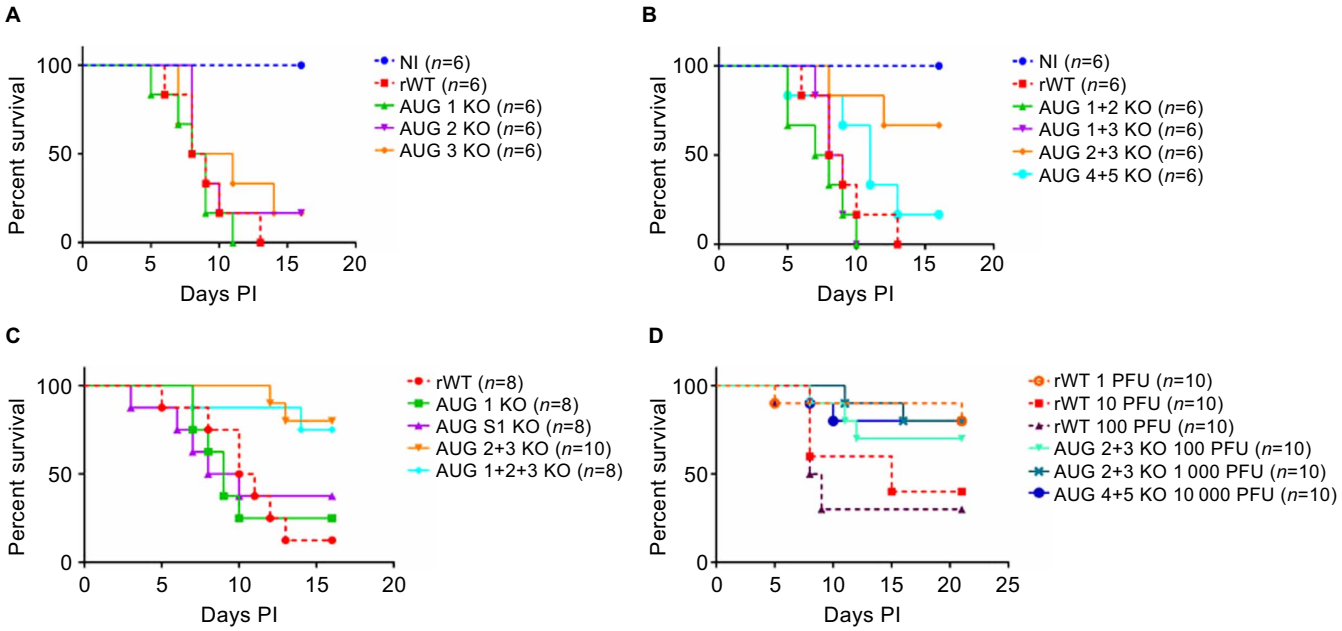

Figure 4 Residual virulence of the AUG KO mutant viruses in C57BL/6 mice. (**A**, **B**) Six 8-week-old C57BL/6 mice were mock-infected (NI) or infected with 100 PFU of rescued WT virus (ZH548) or with 100 PFU of the different AUG KO mutant viruses knocked out for one of the first three in-frame AUG start codons present at the 5′ end of RVFV M segment (**A**) or for two of the five start codons (**B**). Mice were monitored over a period of 3 weeks, but no changes in survival rates were observed after day 14. (**C**) Eight-week-old C57BL/6 mice were infected with 100 PFU of rescued WT virus (ZH548) or with 100 PFU of the AUG 1 KO, AUG S1 KO, AUG 2+3 KO or AUG 1+2+3 KO mutant viruses. (**D**) Survival curve of C57BL/6 mice infected with different doses of rescued WT ZH548 virus or AUG 2+3 KO virus. Eight-week-old C57BL/6 mice were infected with 1, 10 or 100 PFU of rescued WT ZH548 virus or 100, 1000 or 10 000 PFU of the AUG 2+3 KO mutant virus.

requires the concomitant absence of the NSm and P78 proteins, we carried out another animal test under the above-described conditions using a subset of double AUG KO mutant viruses (Figures 1C and 4B). We tested an AUG 1+2 KO mutant lacking both the NSm and P78 proteins as well as mutants AUG 1+3 KO and AUG 2+3 KO to check for a possible compensatory role of an AUG 3-derived expression product. An AUG 4+5 KO mutant virus encoding all five proteins G_N, G_C, P78, NSm and NSm', as in the WT virus, but retaining only three of the five AUGs, served as a control. Infection with neither of the two mutants that abrogated the combined expression of P78 and NSm or NSm′ (AUG 1+2 KO and AUG 1+3 KO) led to an attenuated phenotype. In contrast, the virulence of the AUG 2+3 KO mutant virus was substantially reduced in this experiment, with a survival rate of 66% compared to 0% for the WT virus. These results demonstrated that NSm is a major determinant of RVFV virulence in mice and that NSm′ may function as its substitute.

P78 alone did not seem to have any major impact on the outcome of RVFV infection in mice. To assess a possible introduction of an AUG that would restore P78 expression *in vivo*, another animal test was carried out in which C57BL/6 mice were infected with either rescued WT virus, the original AUG 1 KO virus or the secured AUG S1 KO virus (Figure 4C). The AUG S1 KO virus was associated with a survival rate of 37.5%, which was not significantly different from the 25% survival rate of mice infected with the original AUG 1 KO virus. In addition, blood samples were recovered from the mice infected with the WT and AUG 1 KO viruses (two animals per group), the viruses were amplified in Vero cells, and viral sequences were analyzed by 3′ RACE. No mutation that could restore P78 expression could be detected in any of the animals tested. Residual virulence of the AUG 1+2+3 KO virus was further compared to that of the AUG 2+3 KO mutant virus to assess whether P78 cooperates with the NSm/NSm′ proteins, which should result in increased attenuation of the triple KO virus. Infections by the AUG 1+2+3 KO virus led to 75% survival in infected mice, and infections by the AUG 2+3 KO virus led to 80% survival. These results indicated no significant contribution of the P78 KO to the attenuated phenotype of the AUG 1+2+3 KO mutant virus.

Next, we attempted to estimate the lethal viral dose leading to 50% mortality in mice (LD_{50}) for the AUG 2+3 KO and WT viruses. We infected mice with 1, 10 and 100 PFU of the WT RVFV or 100, 1000 or 10 000 PFU of the AUG 2+3 KO per animal (Figure 4D). In this mouse model, the LD_{50} for WT RVFV was between 1 and 10 PFU. By contrast, no clear correlation between increased inoculum and mortality rates could be observed for the AUG 2+3 KO mutant virus. Furthermore, mortality remained above 50% and fluctuated from approximately 60% to 70%, even when we increased the inoculum over a thousand times with respect to the LD_{50} of the WT virus. These results confirmed that the KOs of NSm and NSm′, which were associated with a change of only two codons, leads to strong attenuation of RVFV in mice.

Murine macrophages but not fibroblasts discriminate the different AUG KO mutant viruses *in vitro*

Two studies that investigated the potential role of the NSm-related proteins in viral growth in infected cell cultures showed no differences whether the proteins were present or not.[27,28] To assess the behavior of the mutant viruses produced in the context of the ZH548 strain, we infected murine L929 fibroblasts with the mutants or the WT virus at a MOI of 0.01 or 3 (Figure 5A). As previously reported, no significant differences could be observed for any of the viruses tested. Because a recent study demonstrated the importance of macrophages in RVFV infection in mice,[37] we further investigated the growth behavior of

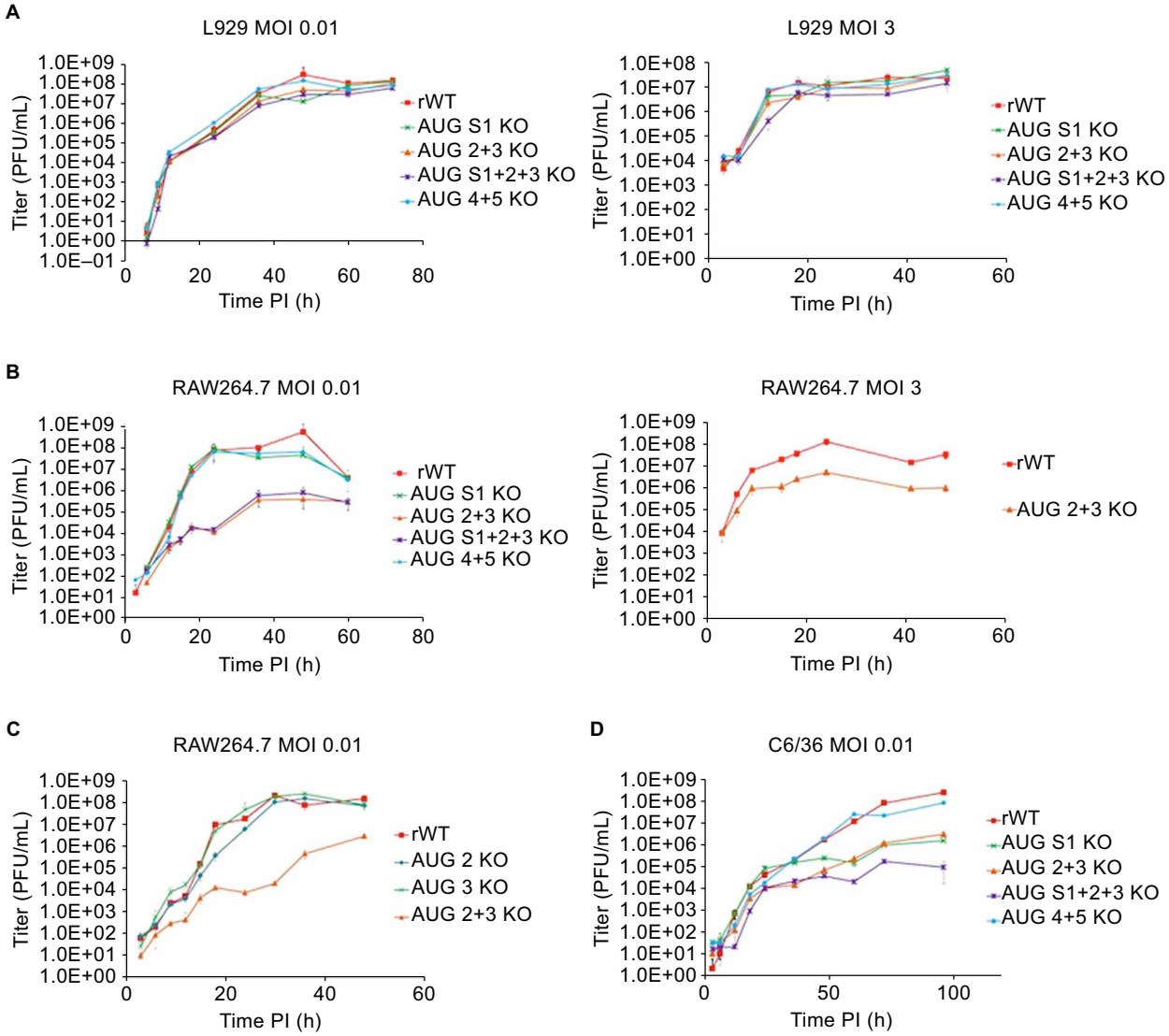

Figure 5 Growth behavior of the selected AUG KO viruses in cell culture. (**A**) Virus production in fibroblasts. L929 cells were infected at an MOI of 0.01 (left panel) or 3 (right panel). Supernatants were harvested at different time points, and virus production was quantified using plaque assays. (**B**, **C**) Virus production in RAW 246.7 cells. Cells were infected at an MOI of 0.01 (**B** left panel, **C**) or 3 (**B** right panel), and virus production was quantified using plaque assays. (**D**) Virus production in C6/36 cells infected at an MOI of 0.01. Virus production was monitored for 96 h PI. All values correspond to the average of a biological triplicate, and the corresponding error bars are reported. Growth curves are representative of several independent experiments.

mutant RVFV at a low MOI of 0.01 in the murine macrophage-like RAW 264.7 cell line (Figure 5B). In this cell type, we observed a 2-log reduction in virus titers for the two mutants that were defective for NSm and NSm' expression, which correlated with the attenuated phenotype in mice. To investigate if this reduction in virus production resulted from a cell-to-cell anti-viral signaling event that primed uninfected cells, the AUG 2+3 KO virus was compared to the WT virus at a MOI of 3, to obtain a synchronized infection of cells, but the growth of the AUG 2+3 KO virus was still significantly reduced (Figure 5B). Furthermore, no apparent cytopathic effects were observed in RAW 264.7 cells infected with the AUG 2+3 KO or AUG S1+2+3 KO viruses. Taken together, these results suggest that, in the absence of NSm/NSm′, infected cells produce an efficient anti-viral response that leads to reduced virus production. To confirm that this phenotype was dependent on the KO of both AUG 2 and 3, as in mice, the AUG 2 KO and AUG 3 KO single mutants were compared to the WT and AUG 2+3 KO viruses in RAW 264.7 cells (Figure 5C). The virus production from the AUG 2 KO or AUG 3 KO mutants was similar to that of the WT virus, demonstrating that expression of NSm or NSm′ alone is sufficient for the virus to efficiently replicate in murine macrophage-like RAW 264.7 cells.

Impact of the M-encoded accessory proteins on virus production in mosquito cells and infectivity in *Aedes aegyti* mosquitoes

Because RVFV is propagated in nature by a mosquito vector, we tested the effect of the NSm-related proteins on virus production in arthropod-derived *Aedes albopictus* cells (C6/36) (Figure 5D). All mutant viruses that lacked one or both forms of the NSm proteins were produced at reduced titers. The AUG S1+2+3 KO virus was the most affected mutant virus, with a 3-log reduction in virus production compared to the WT virus. Mutants AUG S1 KO and AUG 2+3 KO displayed an intermediate phenotype,

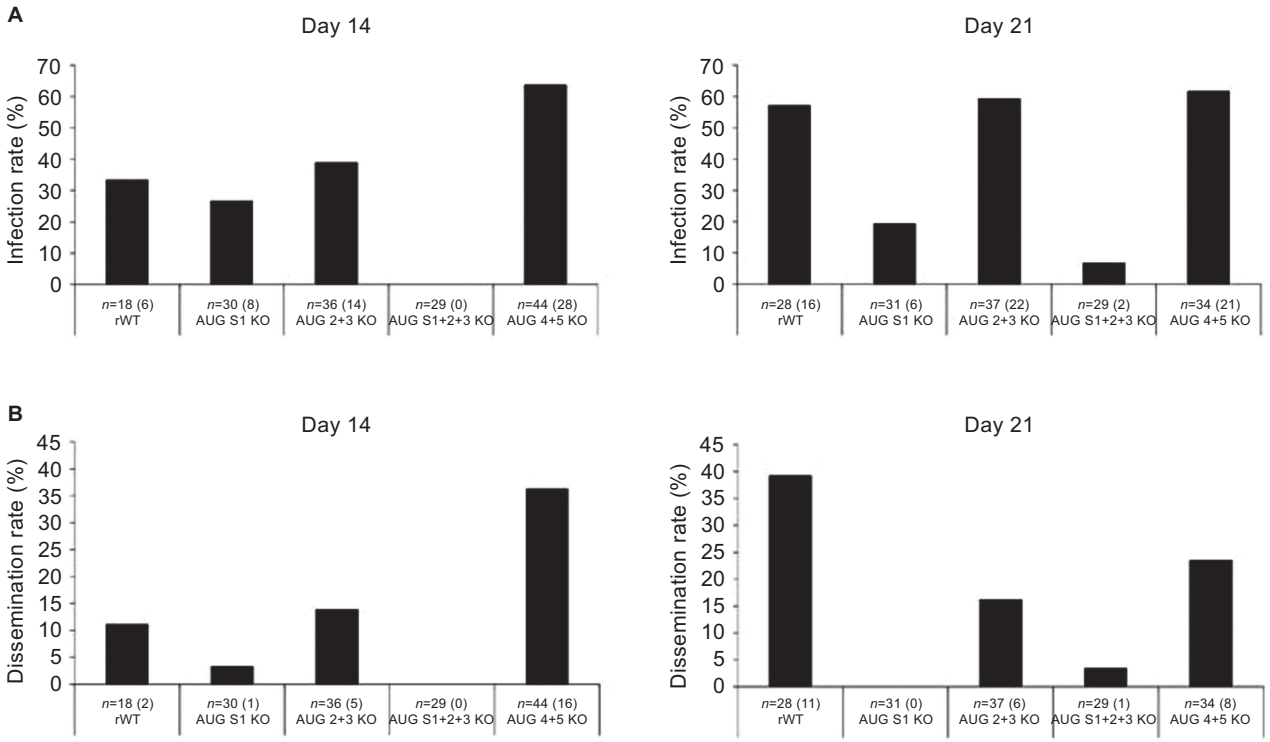

Figure 6 Infection of *Aedes aegypti* mosquitoes by WT and AUG KO mutant viruses. (**A**, **B**) Female *Aedes aegyti* mosquitoes were infected with WT or mutant RVFV by ingestion of blood meals containing preparations of infectious viruses (titer 6.6×10^7 PFU/mL). Viral loads were analyzed in the bodies and heads of the infected mosquitoes using plaque assays on different days PI. (**A**) Infection rates are given as the number of positive bodies divided by the total number of mosquitoes. (**B**) The dissemination rate was calculated from the number of positive heads relative to the total number of mosquitoes. The infection and dissemination rates were analyzed at 14 days PI (left panel) and 21 days PI (right panel).

suggesting a cooperative interaction between P78 and NSm in mosquito cells.

Next, we compared the ability of the different mutant viruses to infect and disseminate successfully within a mosquito vector (Figure 6). *Aedes aegypti* mosquitoes display high infection and dissemination rates after artificial infection with WT RVFV.[38] To this end, *Aedes aegypti* mosquitoes were infected with purified WT or mutant viruses using an artificial feeding system, and the infection by WT virus was compared to those by the AUG S1 KO, AUG 2+3 KO, AUG S1+2+3 KO and AUG 4+5 KO viruses. To determine the infection and dissemination rates, the infectious virus recovered from the body and head of infected mosquitoes 14 and 21 days PI was quantified by plaque assays. Infection and dissemination rates correspond to the ratio of virus-positive bodies or heads, respectively, relative to the total number of mosquitoes tested. We found that the infection rates for the AUG 2+3 KO and AUG 4+5 KO mutant viruses were similar to that of WT virus-infected mosquitoes at days 14 and 21 PI. The infection rate of the AUG S1 KO virus no longer expressing P78 was only reduced at day 21 PI. In contrast, the infection rate for the AUG S1+2+3 KO virus was strongly altered, with 0% and 7% positive mosquitoes on days 14 and 21 PI, respectively, compared to 33% and 57%, respectively, for the WT virus (Figure 6A). These findings are consistent with recent observations of mosquitoes infected with a mutant virus in which the entire NSm region has been deleted.[30]

The dissemination rate of the AUG 2+3 KO virus was very similar to that of the WT virus at day 14 PI, but it did not rise between days 14 and 21 PI, as it did for the WT virus. The KO of P78 markedly affected the ability of the virus to disseminate within infected mosquitoes, as measured by the detection of virus in the head of only one individual. The infection rate of the AUG S1+2+3 KO mutant virus was so low that no conclusion could be drawn regarding its ability to disseminate within a mosquito host (Figure 6B). The dissemination rate of the AUG 4+5 KO virus was increased at day 14 PI and reduced at day 21 PI when compared with the WT virus, although not to the extent of the other mutant viruses. Overall, the NSm-related proteins appeared to modulate virus infectivity in C6/36 cell cultures by distinct and possibly synergistic mechanisms. In mosquitoes, P78 is the major determinant of virus dissemination, while NSm alone only has a minor contribution.

DISCUSSION

Five AUG codons are present in the NSm coding sequence of the RVFV M segment. These AUG codons are alternatively used to produce the two major structural glycoproteins G_N and G_C and at least two accessory proteins NSm and P78, the latter consisting of a fusion between the NSm and G_N proteins. Mutant viruses deleted of the entire NSm region and accordingly lacking expression of NSm and P78 have been shown to be highly attenuated in rats and to be defective for virus spread in mosquitoes.[29–31] In this study, we evaluated the relative contribution of the different NSm-related proteins to RVFV infectivity and virulence in vertebrate and invertebrate species. To this end, one or several of the AUG codons in the NSm region were knocked out in the virulent ZH548 RVFV strain, and mutant viruses were tested for their ability to propagate in mice, a pertinent animal model to study RVFV pathogenesis, and in mosquitoes, the natural vector of RVFV.[36,38,39] In mice, we found that NSm is a major virulence factor, as opposed to P78, which does not seem to have any detectable effect on this model.

However, attenuation of RVFV can only be observed when AUG 2 and AUG 3 are concomitantly knocked out due to expression of a 13-kDa protein, NSm′, from AUG 3 that corresponds to a slightly truncated, functionally active form of NSm. These findings were unexpected because AUG 3 was not considered to contribute significantly to the expression of viral proteins,[19] presumably due to its proximity to AUG 2. However, our results are consistent with the reported anti-apoptotic function of NSm that can be mediated in *trans* using plasmids expressing proteins from AUG 2, and to some extent from AUG 3, of the M segment in cells infected by a mutant RVFV deleted of the entire NSm region.[26] The reason for duplicate functionalities of the NSm protein in the virus is rather unclear. The AUG 3 codon could be located in a more favorable context for protein translation in a particular host or cell type, or the methionine residue encoded by the AUG 3 codon could contribute to a biological property of the NSm protein.

Interestingly, we found that production of mutant viruses lacking NSm and NSm′ expression is strongly reduced in infected RAW 264.7 monocytic cells, whereas the growth of single AUG 2 KO or AUG 3 KO mutant viruses remain comparable to that of the WT virus (Figures 5B and 5C). The interplay between RVFV and macrophages might tightly rely on the identity of the viral strain and the nature of the infected macrophages, as the growth of a mutant virus derived from an attenuated strain of RVFV (MP12) that contains a deletion of the entire NSm region is not affected in J774.1 macrophages.[26] Macrophages have been shown to contribute to RVFV invasion of the central nervous system, and viral antigens can be detected in macrophages present in the liver, pancreas, ovaries and splenic dendritic cells *in vivo*.[37,39–43] Further studies are thus needed to clarify the contribution of macrophages to RVFV pathogenesis and to define the mechanisms by which NSm counteracts host antiviral responses.

The NSm non-structural protein as well as its substitute NSm′ is specifically transported to the surface of mitochondria (Figure 3).[35] The anti-apoptotic activity of NSm requires its proper mitochondrial localization to be effective, and this activity lies within the 45 C-terminal amino acids of the protein.[35] The association of NSm with mitochondria may also be important in regulating the cellular p38 MAPK response.[44] p38 signaling can be triggered through many different stimuli, such as exposure to UV, elevated reactive oxygen species (ROS) or cytokines such as TNF-α or IL-1. In the case of RVFV, p38 activation is triggered by increased levels of ROS, which is regulated at least in part at the level of mitochondria.[44,45] ROS production can be promoted in mitochondria by complex I as part of the respiratory chain.[45] Whether nicotinamide adenine dinucleotide (NADH) dehydrogenase subunit 1, which is a component of complex I and has been identified as a potential cellular partner of the NSm protein,[46] is involved in this process remains to be addressed. Alternatively, NSm could modulate ROS production by interacting with the cytosolic side of mitochondria, as shown for other viral cytoplasmic proteins such as the core protein of hepatitis C virus or the X protein of hepatitis B.[47–49]

A surprising finding is that P78 did not influence RVFV virulence in our mouse model. We expected this protein to play a significant role during virus infection in mice because a mutation that introduced a novel AUG codon upstream of the authentic AUG 1 site and restored P78 protein expression in a mammalian cell culture infected by the AUG 1 KO mutant virus was selected (Supplementary Figures S1). Although we did not observe such a compensatory mutation emerging *in vivo*, we introduced two additional stop codons downstream of the AUG 1 KO (AUG S1 KO virus) to exclude any event that would lead to P78 expression and enhance virus infectivity. The secured AUG S1 KO mutant virus was not attenuated in mice compared to the AUG 1 KO or WT viruses, confirming that P78 is not a determinant of RVFV virulence in a mammalian host infected by the intraperitoneal route (Figure 4C). By contrast, P78 appears as a major determinant of virus dissemination in *Aedes aegypti* mosquitoes, suggesting that this protein is an essential component of the RVFV transmission cycle. Although NSm does not significantly impact virus infectivity in the invertebrate host, in contrast to what has been suggested previously,[31] a cooperative interaction between the P78 and NSm proteins seems to take place during infection of the mosquito vector. The triple KO mutant virus is virtually incapable of replicating in mosquitoes and grows to substantially lower levels in infected mosquito cells compared to the AUG S1 KO or AUG 2+3 KO mutant viruses (Figures 5D and 6).

P78 is a glycoprotein that localizes to the Golgi, where RVFV particles have been shown to assemble prior to their release into the extracellular medium.[20,50] The two potential glycosylation sites that are present in the G_N and NSm sequences have been shown to be modified in P78, an indication that both the NSm and G_N ectodomains are oriented towards the lumen of the endoplasmic reticulum.[51] Such a topology favors a direct interaction between P78 and the G_C molecules processed from the same precursor and is consistent with the rapid detection of a P78/G_C heterodimer in pulse-chase experiments.[21] P78 was initially found to co-sediment with virus or virus-like particles.[22–24] However, a recent study shows that incorporation of large glycoprotein P78 into the virus particle is only observed in C6/36 mosquito cells, suggesting a critical role for this protein in the invertebrate host.[25] Interestingly, the sequence surrounding AUG 1 corresponds more closely to the Kozak consensus sequence of Drosophila than of vertebrates (Table 1)[52] and could perhaps lead to higher expression levels of P78 in arthropod cells infected by RVFV in comparison to infected mammalian cells.

Despite the fact that P78 encompasses the entire amino-acid sequence of NSm, we found that both proteins fulfill fundamentally

Table 1 The nucleotidic context of AUG codons present in the NSm region of the RVFV M segment (adapted from Cavener[52])

	−6	−5	−4	−3	−2	−1	+1	+2	+3	+4
Kozak consensus sequence vertebrate	G	C	C	A/G	C	C	A	U	G	G
Kozak consensus sequence drosophila	A	U	C	A	A	A	A	U	G	A
AUG1	C	A	U	U	A	A	A	U	G	U
AUG2	C	C	A	G	A	G	A	U	G	A
AUG3	G	A	G	G	A	G	A	U	G	C
AUG4	G	A	A	A	C	C	A	U	G	G
AUG5	A	U	U	G	C	A	A	U	G	A

distinct functions to ensure virus propagation in both mosquito and vertebrate hosts. Our results illustrate how arthropod-borne viruses accommodate a wide host range while maintaining a compact genome organization. To face a genomic size constraint, RNA viruses have adopted various strategies to enrich their functional repertoire without exceeding size limits, beyond which their probability of surviving lethal mutations introduced by their error-prone RNA polymerase becomes limited. The use of multiple translation initiation sites situated either in-frame, as for phleboviruses, or in overlapping ORFs, as for orthobunyaviruses and hantaviruses, is one adaptive solution.[53] Gain-of-function mutations, even when they benefit virus replication in only one host species, are maintained during evolution by selective pressure exerted during constant invertebrate/vertebrate transmission cycles.[54,55]

In conclusion, we show that the small cytosolic NSm protein of RVFV is a major virulence factor in the mammalian host and that NSm′ is a functionally active surrogate. A striking finding is that NSm only has a limited effect in the mosquito vector, whereas P78, a protein in which NSm remains fused to G_N and that associates with virus particles, critically influences RVFV dissemination in the invertebrate host. The means by which these proteins facilitate virus spread in different species and whether they cooperate in any way are questions that remain to be addressed.

ACKNOWLEDGEMENTS

The authors acknowledge Agnès Billecocq and Xavier Carnec (Molecular Genetics of Bunyaviruses, Institut Pasteur, France) for their initial help in using the reverse genetics system. The authors also wish to thank Félix Rey (Head of the Structural Virology Unit, Institut Pasteur, France), François Rougeon (Professor Emeritus, Institut Pasteur) and Xavier Montagutelli (Head of the Central Animal Facilities, Institut Pasteur, France) for their support and critical reading of the manuscript. This work was funded by the Agence Nationale de la Recherche (grant NO 11-BSV3-007 01).

1 Daubney R, Hudson JR, Garnham PC. Enzootic hepatitis or rift valley fever. An undescribed virus disease of sheep cattle and man from east africa. *J Pathol Bacteriol* 1931; **34**: 545–579.
2 Findlay GM. Rift valley fever or enzootic hepatitis. *Trans R Soc Trop Med Hyg* 1932; **25**: 229–IN211.
3 Bird BH, Ksiazek TG, Nichol ST, Maclachlan NJ. Rift Valley fever virus. *J Am Vet Med Assoc* 2009; **234**: 883–893.
4 Meegan JM, Hoogstraal H, Moussa MI. An epizootic of Rift Valley fever in Egypt in 1977. *Vet Rec* 1979; **105**: 124–125.
5 Arthur RR, El-Sharkawy MS, Cope SE *et al*. Recurrence of Rift Valley fever in Egypt. *Lancet* 1993; **342**: 1149–1150.
6 Chevalier V, Pepin M, Plee L, Lancelot R. Rift Valley fever—a threat for Europe? *Euro Surveill* 2010; **15**: 19506.
7 Gale P, Brouwer A, Ramnial V *et al*. Assessing the impact of climate change on vector-borne viruses in the EU through the elicitation of expert opinion. *Epidemiol Infect* 2009; **138**: 214–225.
8 Hoogstraal H, Meegan JM, Khalil GM, Adham FK. The Rift Valley fever epizootic in Egypt 1977–78. 2. Ecological and entomological studies. *Trans R Soc Trop Med Hyg* 1979; **73**: 624–629.
9 Madani TA, Al-Mazrou YY, Al-Jeffri MH *et al*. Rift Valley fever epidemic in Saudi Arabia: epidemiological, clinical, and laboratory characteristics. *Clin Infect Dis* 2003; **37**: 1084–1092.
10 Mohamed M, Mosha F, Mghamba J *et al*. Epidemiologic and clinical aspects of a Rift Valley fever outbreak in humans in Tanzania, 2007. *Am J Trop Med Hyg* 2010; **83**: 22–27.
11 Pepin M, Bouloy M, Bird BH, Kemp A, Paweska J. Rift Valley fever virus (Bunyaviridae: Phlebovirus): an update on pathogenesis, molecular epidemiology, vectors, diagnostics and prevention. *Vet Res* 2010; **41**: 61.
12 Laughlin LW, Meegan JM, Strausbaugh LJ, Morens DM, Watten RH. Epidemic Rift Valley fever in Egypt: observations of the spectrum of human illness. *Trans R Soc Trop Med Hyg* 1979; **73**: 630–633.
13 Ikegami T, Makino S. The pathogenesis of Rift Valley fever. *Viruses* 2011; **3**: 493–519.
14 Plyusnin A, Elliott RM. *Bunyaviridae: molecular and cellular biology*. Norfolk: Caister Academic Press, 2011.
15 Ikegami T. Molecular biology and genetic diversity of Rift Valley fever virus. *Antiviral Res* 2012; **95**: 293–310.
16 Schmaljohn CS, Nichol ST. Bunyaviridae. In: Knipe DM, Howley PM (ed.) *Fields virology*. 5th ed. Philadelphia, PA: Lippincott Williams & Wilkins, 2007: 1741–1789.
17 Kakach LT, Wasmoen TL, Collett MS. Rift Valley fever virus M segment: use of recombinant vaccinia viruses to study Phlebovirus gene expression. *J Virol* 1988; **62**: 826–833.
18 Suzich JA, Collett MS. Rift Valley fever virus M segment: cell-free transcription and translation of virus-complementary RNA. *Virology* 1988; **164**: 478–486.
19 Suzich JA, Kakach LT, Collett MS. Expression strategy of a phlebovirus: biogenesis of proteins from the Rift Valley fever virus M segment. *J Virol* 1990; **64**: 1549–1555.
20 Wasmoen TL, Kakach LT, Collett MS. Rift Valley fever virus M segment: cellular localization of M segment-encoded proteins. *Virology* 1988; **166**: 275–280.
21 Gerrard SR, Nichol ST. Synthesis, proteolytic processing and complex formation of N-terminally nested precursor proteins of the Rift Valley fever virus glycoproteins. *Virology* 2007; **357**: 124–133.
22 Kortekaas J, Oreshkova N, Cobos-Jiménez V *et al*. Creation of a nonspreading Rift Valley fever virus. *J Virol* 2011; **85**: 12622–12630.
23 Pichlmair A, Habjan M, Unger H, Weber F. Virus-like particles expressing the nucleocapsid gene as an efficient vaccine against Rift Valley fever virus. *Vector Borne Zoonotic Dis* 2010; **10**: 701–703.
24 Struthers JK, Swanepoel R, Shepherd SP. Protein synthesis in Rift Valley fever virus-infected cells. *Virology* 1984; **134**: 118–124.
25 Weingartl HM, Zhang SZ, Marszal P, McGreevy A, Burton L, Wilson WC. Rift Valley Fever virus incorporates the 78 kDa glycoprotein into virions matured in mosquito C6/36 cells. *PLoS ONE* 2014; **9**: e87385.
26 Won S, Ikegami T, Peters CJ, Makino S. NSm protein of Rift Valley fever virus suppresses virus-induced apoptosis. *J Virol* 2007; **81**: 13335–13345.
27 Gerrard SR, Bird BH, Albarino CG, Nichol ST. The NSm proteins of Rift Valley fever virus are dispensable for maturation, replication and infection. *Virology* 2007; **359**: 459–465.
28 Won S, Ikegami T, Peters CJ, Makino S. NSm and 78-kilodalton proteins of Rift Valley fever virus are nonessential for viral replication in cell culture. *J Virol* 2006; **80**: 8274–8278.
29 Bird BH, Albarino CG, Nichol ST. Rift Valley fever virus lacking NSm proteins retains high virulence *in vivo* and may provide a model of human delayed onset neurologic disease. *Virology* 2007; **362**: 10–15.
30 Crabtree MB, Kent Crockett RJ, Bird BH *et al*. Infection and transmission of Rift Valley fever viruses lacking the NSs and/or NSm genes in mosquitoes: potential role for NSm in mosquito infection. *PLoS Negl Trop Dis* 2012; **6**: e1639.
31 Kading RC, Crabtree MB, Bird BH *et al*. Deletion of the NSm virulence gene of Rift Valley fever virus inhibits virus replication in and dissemination from the midgut of *Aedes aegypti* mosquitoes. *PLoS Negl Trop Dis* 2014; **8**: e2670.
32 Ito N, Takayama-Ito M, Yamada K, Hosokawa J, Sugiyama M, Minamoto N. Improved recovery of rabies virus from cloned cDNA using a vaccinia virus-free reverse genetics system. *Microbiol Immunol* 2003; **47**: 613–617.
33 Billecocq A, Gauliard N, Le May N, Elliott RM, Flick R, Bouloy M. RNA polymerase I-mediated expression of viral RNA for the rescue of infectious virulent and avirulent Rift Valley fever viruses. *Virology* 2008; **378**: 377–384.
34 do Valle TZ, Billecocq A, Guillemot L *et al*. A new mouse model reveals a critical role for host innate immunity in resistance to Rift Valley fever. *J Immunol* 2010; **185**: 6146–6156.
35 Terasaki K, Won S, Makino S. The C-terminal region of Rift Valley fever virus NSm protein targets the protein to the mitochondrial outer membrane and exerts anti-apoptotic function. *J Virol* 2013; **87**: 676–682.
36 Ross TM, Bhardwaj N, Bissel SJ, Hartman AL, Smith DR. Animal models of Rift Valley fever virus infection. *Virus Res* 2012; **163**: 417–423.
37 Gommet C, Billecocq A, Jouvion G *et al*. Tissue tropism and target cells of NSs-deleted rift valley fever virus in live immunodeficient mice. *PLoS Negl Trop Dis* 2011; **5**: e1421.
38 Moutailler S, Krida G, Schaffner F, Vazeille M, Failloux AB. Potential vectors of Rift Valley fever virus in the Mediterranean region. *Vector Borne Zoonotic Dis* 2008; **8**: 749–753.
39 Smith DR. Steele KE, Shamblin J *et al*. The pathogenesis of Rift Valley fever virus in the mouse model. *Virology* 2010; **407**: 256–267.
40 Kamal SA. Pathological studies on postvaccinal reactions of Rift Valley fever in goats. *Virol J* 2009; **6**: 94.
41 McElroy AK, Nichol ST. Rift Valley fever virus inhibits a pro-inflammatory response in experimentally infected human monocyte derived macrophages and a pro-inflammatory cytokine response may be associated with patient survival during natural infection. *Virology* 2011; **422**: 6–12.
42 Reed C, Steele KE, Honko A, Shamblin J, Hensley LE, Smith DR. Ultrastructural study of Rift Valley fever virus in the mouse model. *Virology* 2012; **431**: 58–70.
43 Shieh WJ, Paddock CD, Lederman E *et al*. Pathologic studies on suspect animal and human cases of Rift Valley fever from an outbreak in Eastern Africa, 2006–2007. *Am J Trop Med Hyg* 2010; **83**: 38–42.
44 Narayanan A, Popova T, Turell M *et al*. Alteration in superoxide dismutase 1 causes oxidative stress and p38 MAPK activation following RVFV infection. *PLoS ONE* 2011; **6**: e20354.
45 Murphy MP. How mitochondria produce reactive oxygen species. *Biochem J* 2009; **417**: 1.

46 Engdahl C, Naslund J, Lindgren L, Ahlm C, Bucht G. The Rift Valley Fever virus protein NSm and putative cellular protein interactions. *Virol J* 2012; **9**: 139.
47 Wang T, Campbell RV, Yi MK, Lemon SM, Weinman SA. Role of hepatitis C virus core protein in viral-induced mitochondrial dysfunction. *J Viral Hepat* 2010; **17**: 784–793.
48 Okuda M, Li K, Beard MR *et al*. Mitochondrial injury, oxidative stress, and antioxidant gene expression are induced by hepatitis C virus core protein. *Gastroenterology* 2002; **122**: 366–375.
49 Waris G, Huh KW, Siddiqui A. Mitochondrially associated hepatitis B virus X protein constitutively activates transcription factors STAT-3 and NF-kappa B via oxidative stress. *Mol Cell Biol* 2001; **21**: 7721–7730.
50 Ellis DS, Shirodaria PV, Fleming E, Simpson DI. Morphology and development of Rift Valley fever virus in Vero cell cultures. *J Med Virol* 1988; **24**: 161–174.
51 Kakach LT, Suzich JA, Collett MS. Rift Valley fever virus M segment: phlebovirus expression strategy and protein glycosylation. *Virology* 1989; **170**: 505–510.
52 Cavener DR. Comparison of the consensus sequence flanking translational start sites in *Drosophila* and vertebrates. *Nucleic Acids Res* 1987; **15**: 1353–1361.
53 Firth AE, Brierley I. Non-canonical translation in RNA viruses. *J Gen Virol* 2012; **93**: 1385–1409.
54 Greene IP, Wang E, Deardorff ER, Milleron R, Domingo E, Weaver SC. Effect of alternating passage on adaptation of sindbis virus to vertebrate and invertebrate cells. *J Virol* 2005; **79**: 14253–14260.
55 Moutailler S, Roche B, Thiberge JM, Caro V, Rougeon F, Failloux AB. Host alternation is necessary to maintain the genome stability of rift valley fever virus. *PLoS Negl Trop Dis* 2011; **5**: e1156.

Supplementary Information for this article can be found on *Emerging Microbes and Infections*' website (http://www.nature.com/emi/).

SUPPLEMENTARY INFORMATION

Figure S1: Stability of the AUG 1 KO mutant virus in mammalian cell culture. (**A**) Vero E6 cells were infected with the AUG 1 KO mutant virus at an MOI of 0.01, cell culture supernatants recovered between 72 to 96 h PI were used to infect a new monolayer of Vero E6 cells, this infection cycle was repeated 5 times, and RNA was extracted from the cells at the end of each cycle. RNA was subjected to 3'-RACE followed by RT-PCR to amplify and sequence the 5'-end of the M segment. Sequences from the initial AUG 1 KO virus stock as well as from viruses harvested at passages 4 and 5 are reported in the antigenomic orientation on the respective chromatograms. Sites corresponding to the knocked out AUG 1 (black underlining) and to a stop codon present immediately upstream of the original AUG1 (red underlining) are highlighted. Nucleotide 10 (black box), consisting of a cytosine in the stock preparation but of a uracil in the viral RNA after 5 rounds of infections, is boxed in black. (**B**) Vero E6 cells were infected with wt ZH548 virus or preparations of AUG 1 KO viruses derived from the different passages. P78 was detected by western blotting with anti-NSm Abs in cell lysates recovered at 18 h PI.

Supplementary Figure 1